ELSEVIER

Catalysis Today 77 (2003) 325–333

CATALYSIS TODAY

www.elsevier.com/locate/cattod

Catalytic oxidation of methanol to formaldehyde: an example of kinetics with transport phenomena in a packed-bed reactor

R. Tesser, M. Di Serio, E. Santacesaria*

Dipartimento di Chimica, dell'Università FEDERICO II di Napoli, Via Cinthia, Complesso Monte S. Angelo, 80126 Napoli, Italy

Abstract

In the present work the partial oxidation of methanol to formaldehyde has been studied as an example of strongly exothermic reaction affected by internal diffusion in order to deep the topic of mass and heat transfer in packed-bed catalytic reactors both at particle level, introducing the calculation of the effectiveness factor for complex reactions network, and at reactor level, for what concerns long range gradients of composition and temperature. The aim of the work is to stress the impact of the use of rigorous numerical methods, today possible for the high performances reached by the computers, in the solution of a simultaneous set of many differential equations that are necessary to describe completely the mentioned system. A complete mathematical model of the particle and the reactor is presented and a solution strategy is reported for the chosen reaction by considering a reliable kinetic law and evaluating related parameters from experimental data reported by the literature. Calculation results are reported for both particle internal profiles and reactor simulation. The described approach can easily be extended to many other devices and reactors geometry such as, e.g., the ones used in the field of environmental catalysis.

Keywords: Catalytic oxidation; Methanol; Formaldehyde; Kinetics; Mass transfer; Packed-bed reactors

1. Introduction

A reaction occurring inside a catalytic particle consumes reagents giving products and releasing or consuming heat, according to the reaction is exothermic or endothermic. Therefore, the concentration of the reagents decreases, inside the particle, from external geometric surface to the centre, while, on the contrary, the concentration of the products increases. In the meantime, temperature locally changes, as a consequence of the heat consumed or released by the reaction. The reaction originates the gradients of concentration and temperature and these act as driving forces for mass and heat transfer inside the catalyst particle. Faster is the reaction, steeper are the gradients. For very fast reactions the described effect significantly propagates toward the external part of the particle giving place to other concentration and temperature gradients between the fluid bulk and the catalyst surface. These external gradients, when the fluid flow regime is turbulent, as normally occurs in industrial reactors, are confined in a very thin layer, the boundary layer, surrounding the solid surface, that being quiescent allows mass and heat transfer only with the mechanism of molecular diffusion, that is a relatively slow process. It is opportune to observe that external diffusion and chemical reaction can be considered consecutive steps and consequently their contributions to the observed reaction rates can be separated. The same approach cannot be used for the internal diffusion, occurring simultaneously with chemical reaction. In order to describe the influence of internal diffusion on the reaction rate we need

* Corresponding author. Fax: +390-81-674-026.
E-mail address: santacesaria@chemistry.unina.it (E. Santacesaria).

0920-5861/02/$ – see front matter
PII: S0920-5861(02)00377-2

Nomenclature

b_w	water absorption parameter
C_b	concentration in the bulk
C_i	concentration of component i
C_p	average gas specific heat
C_P	specific heat
C_i^B	concentration of i in the bulk
C_i^P	concentration of i in the particle, concentration inside particle
C_i^S	surface concentration of i
C_P^P	particle specific heat
d_p	particle diameter
D	reactor diameter
D_{a_i}	axial diffusivity
D_{eff}	effective diffusivity
D_i	diffusivity of component i
D_{r_i}	radial diffusivity
D_{eff_i}, D_e	particle effective diffusivity
F	overall molar flow rate
F_i	molar flow rate of i
G	mass flow velocity
h_w	wall heat transfer coefficient
K_a	axial thermal conductivity
K_e	particle thermal conductivity
K_{eff}, K_e	effective thermal conductivity
K_r	radial thermal conductivity
k_1, k_2, k_3	kinetic constants
n, a, b	reaction orders
N_c	number of components
N_R	number of reactions
P	total pressure
P_f	formaldehyde partial pressure
P_m	methanol partial pressure
P_{O_2}	oxygen partial pressure
P_w	water partial pressure
r	particle radial coordinate
R	reactor radius
R_{G_j}	reaction rate (pellet volume)
R_j	reaction rate (fluid volume)
R_P	characteristic length or particle radius
t	time
T	temperature
T_b	bulk temperature
T_B	bulk temperature
T_c	cooling fluid temperature
T_P	temperature inside the particle
T_S	temperature at the surface
Q	overall volumetric flow rate
$\tilde{R}_j$	reaction rate (catalyst mass)
U	overall heat transfer coefficient
v_1, v_2	reaction rate
x	radial coordinate
X_i	fractional conversion
y_i	gas mole fraction
z	axial coordinate
Z	reactor length

Greek symbols

$\gamma_{i,j}$	stoichiometric coefficient
ΔH	heat of reaction
ε_B	void fraction of the solid, bed void fraction
ε_p	void fraction of the particle
η_j	effectiveness factor
ρ	average gas density
ρ_p	particle density

to reproduce concentration and temperature profiles inside the catalyst particles by solving mass and heat balance equations. The subject has largely been treated in many books, reviews and papers [1–16].

When the particles are put in a reactor, such as, e.g., a fixed-bed reactor, long range gradients (axial and radial) can be observed as a consequence of both the average reaction rate in any single particle and the regime of mass and heat flow adopted in the device.

A rather large number of industrial catalytic processes are carried out in fixed-bed reactors that are, usually, large capacity units. The effort is often to realise isothermal conditions, but, very frequently, this ideal condition cannot be reached. On the contrary, when the reactive system involves an equilibrium reaction a single large-diameter reactor, containing packed beds with different height, and operating in adiabatic conditions, is preferred, because, it is possible to control the overall conversion through the temperature of the outlet flow stream. Therefore, for what concerns the heat transfer, we have two ideal limit conditions that are: the isothermal one, occurring when the heat exchange at the reactor wall is very efficient; the adiabatic regime, where heat exchange is very poor. The

intermediate condition, not isothermal and not adiabatic, is the most frequently encountered in the common practice and we will deal with this more complex situation by facing a significant example of industrial interest.

The complexity of the problem can be better understood keeping into account that the problem have to be solved simultaneously both at a local level, obtaining particle profiles and effectiveness factors for complex reactions network, and at a reactor level reproducing the long-range profiles. This means that, virtually in each point of the catalytic bed, an effectiveness factor calculation must be performed at the conditions valid in that point itself. Many books, papers and reviews have been devoted also to this subject [1–16] even if the treatment of the effectiveness factor calculation for complex reactions network is rarely encountered. A general approach of this type can easily be extended also to devices currently used in environmental catalysis such as, e.g., monolithic reactors.

In this paper the reaction of methanol oxidation to formaldehyde occurring in a tubular packed-bed reactor is considered. This reaction is strongly exothermic and all the before mentioned mass and heat transfer phenomena occur greatly affecting the reaction rates. In order to solve the problem we need a reliable intrinsic kinetic law based on acceptable reaction mechanism [18]. A re-evaluation of literature experimental data have been performed for the determination of the kinetic parameters appearing in the kinetic law [18].

A revisiting of the mentioned reaction is justified considering the exponential development of the computer performances available today that allows a more rigorous approach to the solution of the differential equations involved in the description of the kinetics with mass transfer in a strongly exothermic complex reaction such as the one here considered.

2. Effectiveness factor for complex reactions

In the conversion of methanol to formaldehyde, catalysed by iron–molybdenum oxide catalyst, two consecutive reactions occur that are

$$CH_3OH + \tfrac{1}{2}O_2 \rightarrow CH_2O + H_2O,$$
$$CH_2O + \tfrac{1}{2}O_2 \rightarrow CO + H_2O \qquad (1)$$

Table 1
Physico-chemical data for the calculation of effectiveness factor

$K_e = 2.72 \times 10^{-4}$ kJ/s m K	Effective thermal conductivity
$D_e = 1.07 \times 10^{-5} \exp(-672/T)$ m^2/s	Effective diffusivity
$\rho_P = 1000$ kg/m^3	Particle density
$C_p = 2.5$ kJ/mol K	Particle specific heat
$P = 1.10$ atm	Total pressure
$T_S = 563$ K	Surface temperature
$d_P = 3.0 \times 10^{-3}$ m	Particle diameter
Bulk gas composition (mol%)	
CH_3OH	8.0
CH_2O	1.0
CO	0.0
O_2	16.0
H_2O	0.0
N_2	75.0

The conditions for the reaction, together with catalyst characteristics and other physical parameters, are reported in Table 1 [20].

These reactions are universally recognised to follow a redox-mechanism and the more reliable kinetics is the one suggested by Mars and Van Krevelen [17], i.e.

$$v_1 = \frac{k_1 k_2 P_m^a P_{O_2}^b}{k_1 P_m^a + k_2 P_{O_2}^b} \qquad (2)$$

Different values of a and b have been reported by the literature, generally considering, e.g., $a = b = 1/2$ [21] or $a = 1$, $b = 1/2$ [22]. The last values are more adherent to the Mars–Van Krevelen mechanism in which oxygen is adsorbed by dissociation.

The inhibition induced by the water formed in both the reactions can also be considered by introducing a Langmuir–Hinshelwood term, such as [18,19]:

$$v_1 = \frac{k_1 k_2 P_m^a P_{O_2}^b}{k_1 P_m^a + k_2 P_{O_2}^b} \left(\frac{1}{1 + b_w P_w} \right) \qquad (3)$$

The rate law for the second reaction, has been assumed, in agreement with Dente et al. [20] to be of pseudo-first-order with respect to formaldehyde, i.e.

$$v_2 = k_3 P_f \qquad (4)$$

We adopted the most reliable relationship (3) by recalculating kinetic parameters on the basis of the experimental data published by Dente et al. [20] (see Table 2). It must be pointed out that this kinetic

Table 2
Kinetic parameters for the model

$k_1 = \exp(-18.4586 + 64790/RT)$
$k_2 = \exp(-15.2687 + 57266/RT)$
$b_w = \exp(+21.2814 - 111600/RT)$
$\Delta H_1 = 158.8\,\text{kJ/mol}$
$\Delta H_2 = 238.3\,\text{kJ/mol}$

equation gives quite similar performances in describing kinetic runs as it can be seen in Table 3, but has the advantage of both retaining physical mean and describing the inhibition effect of water becoming important for high conversion degrees, as it has been shown by Santacesaria et al. [18].

For the description of this system, at particle level, a general definition of the effectiveness factor have to be introduced, considering that, for an N_r reactions system we can write an expression of the effectiveness factor related to reaction j of the type

$$\eta_j = \frac{\int_0^{R_P} 4\pi r^2 v_j(C_i, T)\,\mathrm{d}r}{(4/3)\pi R_P^3 v_j(C_i^S, T_S)} \tag{5}$$

The evaluation of the integral in expression (5) involves the determination of temperature and concentration profile inside the catalytic particle by solving material and energy balance. Such balance equations, for steady state conditions, can be written, according to [21], by taking into account for multiple reaction and for multicomponent system constituted by N_c chemical species

$$D_{\text{eff}_i}\left[\frac{\partial^2 C_i^P}{\partial r^2} + \frac{2}{r}\frac{\partial C_i^P}{\partial r}\right] = \rho_P \sum_{j=1}^{N_r} \gamma_{i,j} v_j, \quad i = 1, 2, \ldots, N_c \tag{6}$$

$$K_{\text{eff}}\left[\frac{\partial^2 T_P}{\partial r^2} + \frac{2}{r}\frac{\partial T_P}{\partial r}\right] = \rho_P \sum_{j=1}^{N_r} (-\Delta H_j) v_j \tag{7}$$

The simultaneous solution of this system of partial differential equations must be accomplished using the following boundary conditions:

$$\frac{\partial C_i^P}{\partial r} = 0, \qquad \frac{\partial T_P}{\partial r} = 0 \quad \text{at } r = 0,$$
$$C_i^P = C_i^S, \qquad T_P = T_S \quad \text{at } r = R_P \tag{8}$$

This model, describing the simultaneous diffusion and reaction inside the pellets, constitute a coupled set of one-dimensional boundary value problem that can be solved employing different numerical techniques that can easily be found in the literature (finite difference, orthogonal collocation, etc.). The approach used here is the methods of lines [21], consisting in the conversion of the partial differential equations, represented by the relations (6) and (7), in a system of ordinary differential equations (ODEs). The starting point of this method is a transient form of relations (6) and (7) written as it follows:

$$\varepsilon_P \frac{\partial C_i^P}{\partial t} = D_{\text{eff}_i}\left[\frac{\partial^2 C_i^P}{\partial r^2} + \frac{2}{r}\frac{\partial C_i^P}{\partial r}\right] - \rho_P \sum_{j=1}^{N_r} \gamma_{i,j} v_j \tag{9}$$

$$\varepsilon_P \rho_P C_P^P \frac{\partial T_P}{\partial t} = K_{\text{eff}}\left[\frac{\partial^2 T_P}{\partial r^2} + \frac{2}{r}\frac{\partial T_P}{\partial r}\right] - \rho_P \sum_{j=1}^{N_r} (-\Delta H_j) v_j \tag{10}$$

The subsequent step, consists in the discretisation of the spatial coordinate (particle radius) by choosing a series of internal node point from $r = 0$ to $r = R_P$

Table 3
Comparison between Eq. (2) with $a = b = 1/2$ and Eq. (3) with $a = 1$, $b = 1/2$ for experimental data of Dente et al. [20]

Temperature (°C)	Number of runs	$a = b = 1/2$		$a = 1$, $b = 1/2$	
		Mean error on conversion	Correlation coefficient	Mean error on conversion	Correlation coefficient
220	27	8.96	0.920	11.30	0.912
250	29	5.91	0.952	7.17	0.960
270	20	7.37	0.997	7.49	0.992
300	17	12.64	0.973	12.94	0.973

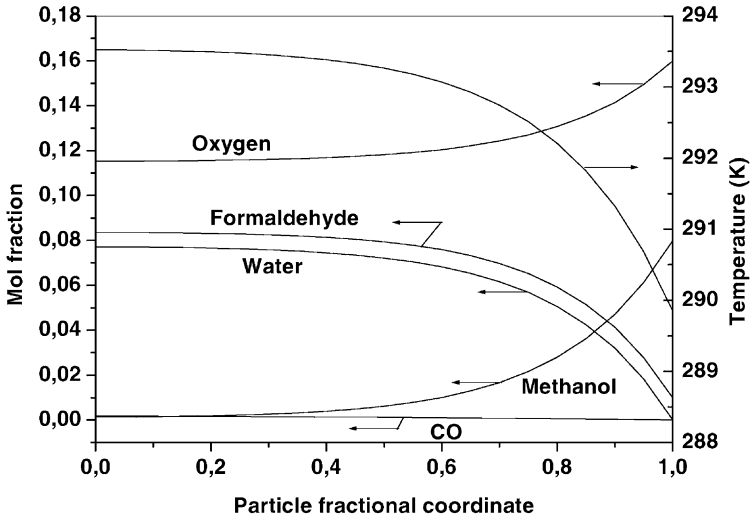

Fig. 1. Concentration and temperature profiles inside catalytic particle.

and replacing the spatial derivatives in Eqs. (9) and (10) with a finite difference approximation. The resulting set of ODEs can be integrated forward in time until reaching stationary conditions representing the steady state solution of Eqs. (6) and (7). This method is preferred for the large availability of efficient ODE integrators and for the less problems of numerical stability, with respect to other solution methods such as finite differences. The advantage of the method of lines becomes evident when the formulation of the model results in a "stiff" system that can be correctly treated by the common ODE solvers such GEAR or LSODE [22].

The application of the model represented by Eqs. (9) and (10) to the considered example (Table 1), is performed with the following assumptions:

- Catalytic particles are spherical and with uniform reactivity, density and thermal conductivity.
- Negligible variation of heat of reactions with the temperature.
- Negligible external resistance so that surface concentration is equal to that of the bulk.
- Equal effective diffusivity for all the chemical species involved.

For what concern the numerical solution implemented we have considered a number of internal points, for particle radius discretisation, equal to $N_n = 20$. This means that, for our system of six components, we have $(N_c + 1) \times N_n = 140$ ODEs to integrate until a stationary state is reached. A further increase in the number of interior points yields a negligible variation in the calculated values for the effectiveness factors. As a result for this calculation we obtain, for each component, the concentration profile inside a catalytic particle as shown in Fig. 1. From this diagram it is evident that for methanol and oxygen, being reagents, the profile decrease from external surface to the centre of the pellet, while, for products, the trend is opposite.

From these profiles it is possible to evaluate the effectiveness factors, for each reaction, employing relation (5) and the results are

$$\eta_1 = 0.38, \qquad \eta_2 = 5.94$$

The high value obtained for the second reaction can be attributed to the low concentration of formaldehyde in the bulk gas, while in the interior of the particle this value is significantly higher resulting in an increasing reaction rate from the surface to the centre of the particle.

As a further result of the illustrated analysis, there is the temperature profile also reported in Fig. 1. Being the reactions exothermic, the temperature increases, as expected, moving from the external surface to the centre and the overall ΔT is about 3.5 K.

3. Reactor profile calculation: an example of non-isothermal and non-adiabatic system

The reaction of methanol conversion to formaldehyde, described in the previous section, has been considered also as an example of the approach to the reactor-level problem. The reactor behaviour can be interpreted starting from the general conservation relations for mass and energy that, for a fixed-bed reactor in which occur N_r chemical reactions involving N_c components, can be written as follows [23]:

$$\varepsilon_B \frac{\partial C_i^B}{\partial t} + v\frac{\partial C_i^B}{\partial z} - D_{a_i}\frac{\partial^2 C_i^B}{\partial z^2} - D_{r_i}\left[\frac{\partial^2 C_i^B}{\partial x^2} + \frac{1}{x}\frac{\partial C_i^B}{\partial x}\right] = (1-\varepsilon_B)\sum_{j=1}^{N_R}\gamma_{i,j}R_{G_j}, \quad i = 1, 2, \ldots N_c \tag{11a}$$

$$\varepsilon_B \frac{\partial T_B}{\partial t} + v\frac{\partial T_B}{\partial z} - K_a\frac{\partial^2 T_B}{\partial z^2} - K_r\left[\frac{\partial^2 T_B}{\partial x^2} + \frac{1}{x}\frac{\partial T_B}{\partial x}\right] = \frac{1-\varepsilon_B}{\rho C_p}\sum_{j=1}^{N_R}(-\Delta H_j)R_{G_j} \tag{11b}$$

Eqs. (11a) and (11b) constitute a set of coupled partial differential equations that must be solved keeping into account for some suitable boundary conditions relative to variables and their derivatives. Usual boundary conditions can be written in the following form:

$$\frac{\partial T_B}{\partial x} = \frac{\partial C_i^B}{\partial x} = 0 \text{ at the centerline of the reactor } (x = 0) \text{ for all } z \tag{12}$$

$$\frac{\partial C_i^B}{\partial r} = 0,$$

$$h_w(T_B - T_C) = -\rho C_p K_r \frac{\partial T_B}{\partial r} \text{ at the wall of reactor } (x = R) \text{ for all } z \tag{13}$$

The first boundary condition (Eq. (12)) results from symmetry consideration around the centreline of a tubular reactor, while the second one (Eq. (13)) is related to the fact that no reactant transport take place across the reactor wall and that the heat transferred to the cooling medium, whose temperature is T_c, is equal to the heat conducted at the wall.

For what concerns axial boundary conditions, at the reactor inlet, we can write the following relations:

$$(vC_i^B)_{in} = \left(vC_i^B - D_{a_i}\frac{\partial C_i^B}{\partial z}\right)_{z=0},$$

$$(vT_B)_{in} = \left(vT_B - K_a\frac{\partial T_B}{\partial z}\right)_{z=0} \quad \text{at } z = 0 \tag{14}$$

and for the outlet

$$\frac{\partial C_i^B}{\partial z} = \frac{\partial T_B}{\partial z} = 0 \quad \text{at } z = Z \tag{15}$$

The above mentioned boundary conditions are based on the continuity of the flux (mass or heat) across a boundary represented by the catalytic bed inlet and outlet.

The complete bidimensional model represented by relations (11a) and (11b) can be simplified in order to obtain a practical solution to the problem, mainly by neglecting the effect of radial profiles.

In Table 4 are reported the characteristics of the reactor and the adopted operating conditions taken from [24,25]. By using these conditions and the kinetic data reported in Table 2, we have performed a simulation of the reactor behaviour in terms of temperature profile along the axis. In this case, a further complication must be introduced in the framework of the model, consisting in the calculation of the effectiveness factor along the reactor, taking into account diffusion limitations inside the particles.

The basic assumptions adopted here, for the model simplifications, can be summarised in the following points:

- No axial and radial dispersion.
- No radial temperature and concentration gradients in the reactor tube.
- Plug flow through the reactor.

For what concerns radial profiles, according to the criteria reported in [23], they can be considered negligible in the case of a radial aspect ratio $m = R/d_P = 2.5$ that is below the limit value of 4. Considering these assumptions, it is evident that the resulting model is mono-dimensional, because, takes into account only for axial or longitudinal profiles along the reactor. In each point of the axial coordinate, an effectiveness factor calculation is performed in order to obtain a reaction rate operative in that point and determining a

Table 4
Reactor characteristic and operating conditions

	Run 1 [24]	Run 3 [24]	Run S4 [25]
Inlet temperature (K)	569	562	577
Inlet molar flow rate (kmol/s)	0.506×10^{-5}	1.249×10^{-5}	0.968×10^{-5}
Total pressure (atm)	1.09	1.25	1.17
Bulk density of the bed (kg/m^3)	1000	1000	1000
Overall heat transfer coefficient, U (kJ/m^2 s K)	0.072	0.14	0.11
Heating medium temperature (K)	554	555	559
Reactor diameter (m)	0.015	0.015	0.015
Particles diameter (m)	3.0×10^{-3}	3.0×10^{-3}	3.0×10^{-3}
Reactor length (m)	0.60	0.60	0.60
Gas inlet composition (mol%)			
CH_3OH	3.31	3.03	7.12
O_2	20.30	20.35	19.50
N_2	76.39	76.62	73.38

profile also for the effectiveness factors. On the basis of the exposed assumptions and introducing molar flow rate relative to each component, material balance can be expressed by the following model relations:

$$\frac{\mathrm{d}F_i}{\mathrm{d}z} = \rho_\mathrm{B}\frac{\pi D^2}{4}\sum_{j=1}^{N_\mathrm{r}}\gamma_{i,j}\bar{R}_j, \quad i = 1, 2, \ldots, N_\mathrm{c} \qquad (16)$$

that can be derived upon the following substitution in Eq. (11a):

$$v = \frac{Q}{A}, \qquad QC_i = F_i, \qquad A = \frac{\pi D^2}{4} \qquad (17)$$

The energy balance, represented by relation (11b), have to be simplified, as done for the material balance, according to the assumed absence of radial profiles

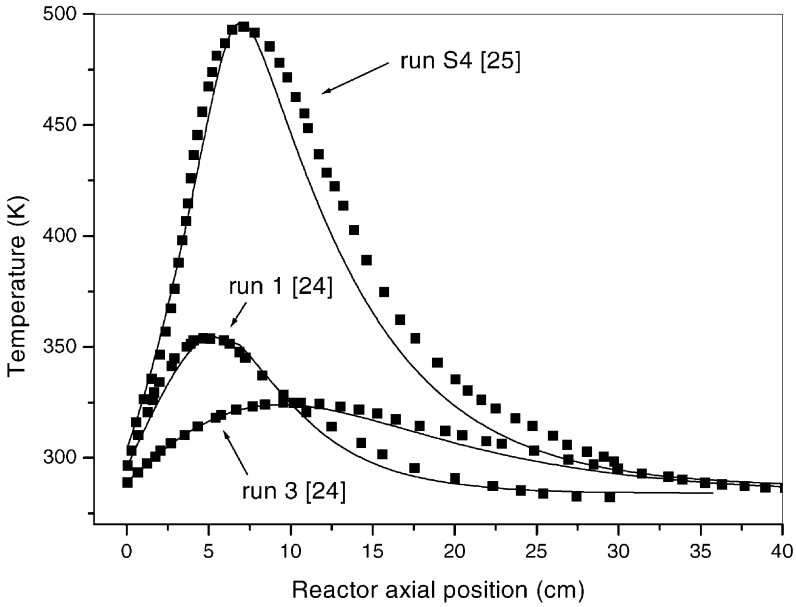

Fig. 2. Axial temperature profiles for different experimental runs.

and to the presence of cooling fluid. The heat transferred across the external surface, per unit of reactor volume, can be defined as it follows:

$$q = \frac{U(T_C - T)\pi D\,dz}{A\,dz} \quad (18)$$

This term must be added algebrically, in the balance equation, to the heat associated with the reaction, yielding the following expression:

$$\left(\sum_{i=1}^{N_c} F_i C_{P_i}\right)\frac{dT}{dz} = \frac{\pi D^2}{4}\rho_B \sum_{j=1}^{N_r}(-\Delta H_j)\bar{R}_j + \pi DU(T_C - T) \quad (19)$$

The set of $N_c + 1$ ordinary differential equations (18) and (19) can be integrated along z-direction to obtain the desired profiles of temperature and concentration. At each integration step along the axis of the reactor, the effectiveness factor for each reaction must be determined employing the relations 5–10. The adopted algorithm for axial integration is that of Runge–Kutta with a variable z step size, inversely proportional to the quantity dT/dz, so that a smaller step size results when the temperature variation increase corresponding to a steeper profile. The main result for this calculation is the temperature profile along the reactor, reported in Fig. 2 for runs 1 and 2 from [24] and for run S4 from [25]. From this figure it is evident that, when the reaction mixture enters the reactor, the gas temperature increases rapidly due to the exothermic nature of the reactive system. As the methanol is consumed the main reaction rate begin to decrease and the same trend is shown by the temperature.

It is interesting to observe that employing the kinetics expressed by relation (3) the mono-dimensional model is able to reproduce with good accuracy also the run S4, that is performed in conditions of apparent parametric sensitivity [25], without the necessity to introduce further complication in the model such as axial dispersion term and radial temperature profile adopted in the original work.

4. Conclusions

In present work, the kinetics with mass transfer of the reaction of methanol oxidation to formaldehyde has been studied starting from experimental data reported from the literature. A rigorous numerical approach has been used to describe the temperature and concentrations profiles of reagents and products either inside the catalyst particles or along the reactor. A reliable Mars and Van Krevelen kinetic law has been adopted also considering the depressing effect of water. The experimental results in the used reactor suggests that radial profiles are negligible and a mono-dimensional model is enough to describe all the runs performed in a tubular reactor by simulating the experimental temperature profiles and outlet composition. It is interesting to observe that the effectiveness factor for the secondary reaction of formaldehyde oxidation is much greater than one because the concentration of this product inside the particle is greater than on the particle surface and reaction rate is consequently higher. In this paper we have shown the opportunity of revisiting old published data in order to remove the excessive model simplifications imposed at that time by the limitation of the computer power calculation.

References

[1] G.F. Froment, K.B. Bishoff, Chemical Reactor Analysis and Design, Wiley, New York, 1990.
[2] J.M. Smith, Chemical Engineering Kinetics, McGraw-Hill, New York, 1981.
[3] H.S. Fogler, Elements of Chemical Reaction Engineering, Prentice-Hall, Englewood Cliffs, NJ, 1986.
[4] J. Horak, J. Pasek, Design of Industrial Chemical Reactors from Laboratory Data, Heyden, London, 1978.
[5] C.N. Satterfield, T.K. Sherwood, The Role of Diffusion in Catalysis, Addison-Wesley, Reading, MA, 1963.
[6] O. Levenspiel, The Chemical Reactor Omnibook, OSU Book Store, Oregon, 1984.
[7] C.N. Satterfield, Heterogeneous Catalysis in Practice, Addison-Wesley, Reading, MA, 1972.
[8] C.D. Holland, R.G. Anthony, Fundamentals of Chemical Reaction Engineering, Prentice-Hall, London, 1979.
[9] S. Carrà, L. Forni, Aspetti Cinetici della Teoria del Reattore Chimico, Tamburini Ed., 1974.
[10] L. Forni, Fenomeni di Trasporto, Cortina Ed., 1979.
[11] M. Dente, E. Ranzi, Principi di Ingegneria Chimica, CLUP, 1976.
[12] J.M. Winterbottom, M.B. King, Reactor Design for Chemical Engineers, Stanley Thorius Ltd., 1999.
[13] A. Wheeler, Reaction Rates and Selectivity in Catalyst Pores, Advances in Catalysis, vol. III, Academic Press, New York, 1951.

[14] R.B. Bird, W.E. Stewart, E.N. Lightfoot, Fenomeni di Trasporto, Case Ed., Ambrosiana, 1970.
[15] R.W. Missen, C.A. Mims, B.A. Saville, Chemical Reaction Engineering and Kinetics, Wiley, New York, 1999.
[16] J.J. Carberry, Chemical and Catalytic Reaction Engineering, McGraw Hill, New York, 1976.
[17] J. Mars, D.W. Van Krevelen, Chem. Eng. Sci. Spec. Suppl. 3 (41), 1954.
[18] E. Santacesaria, M. Morbidelli, S. Carrà, Kinetics of the catalytic oxidation of methanol to formaldehyde, Chem. Eng. Sci. 36 (5) (1981) 909–918.
[19] E.S. Carrà, M.P. Forzatti, Engineering aspects of selective hydrocarbons oxidation, Catal. Rev. Sci. Eng. 15 (1) (1977) 1–52.
[20] M. Dente, R. Poppi, I. Pasquon, Cinetica dell'Ossidazione del Metanolo a Formaldeide con Catalizzatore a base di Ossidi di Fe e Mo. Nota I, La Chimica e l'Industria 46 (11) (1964) 1326–1336.
[21] J.B. Riggs, Introduction to Numerical Methods for Chemical Engineers, Texas Technical University Press, Texas, 1988.
[22] A.C. Hindmarsh, LSODE and LSODI, two initial value ordinary differential equation solvers, ACM-SIGNUM Newslett. 15 (4) 1980.
[23] H.H. Lee, Heterogeneous Reactors Design, Butterworths, London, 1984.
[24] M. Dente, A. Collina, Verifica di un Reattore Tubolare per l'Ossidazione del Metanolo a Formaldeide, La Chimica e l'Industria 48 (6) (1966) 581–588.
[25] M. Dente, A. Collina, Problemi di Verifica di un Reattore Monotubolare in Condizioni di Sensitività Parametrica, Ing. Chim. Ital. 2 (4) (1966) 97–105.